Int. J. Heat Mass Transfer. Vol. 35, No. 11, pp. 2911–2920, 1992
Printed in Great Britain

0017–9310/92 $5.00 + 0.00

Thermal contact resistance across pressed metal contacts in a vacuum environment

T. McWAID† and E. MARSCHALL
Department of Mechanical Engineering, University of California, Santa Barbara, CA 93106, U.S.A.

(*Received* 7 *March* 1991 *and in final form* 10 *December* 1991)

Abstract—The thermal contact conductance has been measured as a function of contact pressure across ten pairs of surfaces in a vacuum environment. A modified version of the Greenwood and Williamson elastic contact model has been used to predict the contact conductance as a function of contact pressure for each pair of specimens. The measured and predicted values have been presented and compared. The predicted values are generally within about 25% of the measured values for isotropically rough surfaces, and within about 50% of strongly anisotropic surfaces. Thus, the theory presented herein constitutes a viable tool for the heat transfer analyst. The theory is relatively easy to implement and the results are reasonably accurate.

INTRODUCTION

THERMAL contact resistance (TCR) results because the actual contact area between two contacting solids is only a small fraction of the nominal contact area. The actual contact area is, in general, comprised of many microcontacts distributed across the nominal contact area.

In the absence of heat transfer via the interstitial medium and heat transfer by radiation, all of the heat flow across a pressed contact must occur across the distributed microcontacts. The resulting concentration of flux lines is manifested in the observed temperature drop across the pressed contact.

Many researchers have investigated thermal contact resistance. Fletcher *et al.* [1, 2] have summarized most of the recent work.

Yovanovich *et al.* [3, 4] have made a large contribution to the field. They assume that contacting asperities undergo purely plastic deformation; the Vicker's micro-hardness is used to relate the actual contact area to the applied pressure. The relations developed by Yovanovich and his co-workers have been used to predict the contact conductance across a pressed contact fairly accurately.

In reality the deformation mode is neither purely plastic nor purely elastic. One might expect that a large degree of plastic deformation would be associated with the first load cycle seen by the contacts; however, the deformation must tend toward fully elastic if the loading is cycled. The goal of this research was to test an elastic contact model for the determination of the parameters required for the prediction of the contact resistance.

In order to predict the TCR across a given pressed contact one must be able to predict the number and average size of the many microcontacts that comprise the actual contact area. Contact models have been developed for this purpose. Greenwood and Williamson proposed one of the first contact models to incorporate the statistical nature of real (rough) surfaces [5].

McCool has recently modified the GW model [6]. The modified GW model has been utilized to obtain the contact parameters necessary for the prediction of the thermal contact resistance across pressed metal contacts in a vacuum environment. The predicted TCR values have been compared to measured TCR values for ten pairs of pressed contacts.

This paper summarizes both the theoretical and experimental aspects of this work. Contact resistance is summarized first. A very brief thermal analysis is presented next; from this analysis we will determine which contact parameters are required in order to predict the thermal contact resistance across a pressed metal contact in a vacuum environment. The modified GW contact model is then summarized. The experimental apparatus and procedure is discussed in the following section. Some of the predicted and measured values of TCR are then presented and compared. Finally, a brief discussion of the uncertainty associated with the experimental values of TCR is presented.

The predicted values are generally within about 25% of the measured values for isotropically rough surfaces, and within about 50% for strongly anisotropic surfaces. Thus, the modified GW contact model can be used to obtain the contact parameters required for the relatively accurate prediction of the

† Presently with the National Institute of Standards and Technology, Precision Engineering Division, Gaithersburg, MD 20899, U.S.A.

NOMENCLATURE

a	contact radius	r	mean summit radius
A_a	actual area of contact	R	thermal contact resistance based on heat flow
A_n	nominal contact area	R'	thermal contact resistance based on heat flux
b	flux tube radius	R_c	constriction resistance for single contact
c	constriction ratio	ΔT	temperature difference across interface
C	contact conductance	W	applied compression force
d	mean plane separation	z_s	difference between summit height and mean surface height.
D_{sum}	density of summits		
E^*	equivalent Young's modulus	Greek symbols	
$g(c)$	constriction alleviation factor	α	bandwidth parameter
k	thermal conductivity	κ_m	mean summit curvature
m_i	moments of power spectral density	σ_s	standard deviation of summit height distribution.
N	number of contact spots		
P	contact pressure		
q	heat flux		
Q	heat flow		

TCR across a pressed metal contact in a vacuum environment.

THERMAL ANALYSIS

Heat transfer through two contacting bodies is characterized by a temperature drop across the interface. Thermal contact resistance is defined as the ratio of the temperature drop across the interface to the heat flow across the interface:

$$R = \frac{\Delta T}{Q} [\mathrm{K\,W^{-1}}]. \tag{1}$$

In the past the contact resistance has sometimes been defined as the ratio of the heat *flux* to the temperature drop across an interface [1, 7, 8]. Resistance values based on the heat flux allow the comparison of data obtained using different geometric configurations, and for the estimation of the resistance across a given mechanical joint. The superscript ′ will be used throughout this paper to denote a resistance (or conductance) based on the heat flux. This same convention has been used by Snaith *et al.* [9].

It is sometimes more convenient to consider the contact conductance rather than the contact resistance across a pressed contact. In general, the conductance equals the inverse of the resistance.

As was alluded to in the Introduction, there are, in general, three modes of heat transfer across a pressed contact. Energy can be transferred by radiation, by conduction through the interstitial medium and by conduction through the microcontacts.

By restricting our discussion to include only pressed contacts at relatively low temperatures (<500 K) located within a vacuum environment ($<10^{-3}$ Torr), we can force essentially all the heat transfer across the pressed contacts to occur via conduction through the actual contact area [10–13]. Henceforth these restrictions will be imposed.

Roess [14] and Mikic and Rohsenow [15] independently determined the total constriction resistance for a singular isothermal contact spot at the center of the apparent contact area. Both derived approximate relations for the constriction resistance by replacing the isothermal contact boundary condition at the contacts with a heat flux boundary condition. The assumed distribution of heat flux ensured that the contacts were nearly isothermal; moreover, the revised boundary conditions allowed an exact solution of the governing partial differential equation.

The results obtained by Roess and Mikic, although expressed in different forms, agree well. The general form of the solution is:

$$R_c = \frac{g(c)}{2ak} \tag{2}$$

where c is the constriction ratio, defined as the ratio of the contact radius to the flux tube radius ($=a/b$), and $g(c)$ is the constriction alleviation factor. Note that equation (2) includes the constriction resistance on both sides of the contact; moreover, the contact plane has been assumed to be a plane of symmetry.

The leap from a consideration of individual contacts to that of contacting surfaces is made by assuming that the contact areas are 'appropriately distributed' [16] across the nominal contact area. An appropriate distribution is one in which neighboring flux tubes do not interact. Each contact feeds a particular flux tube, independent of the neighboring contacts.

In this case [16],

$$g(\bar{c}) \cong (1-\bar{c})^{1.5}, \tag{3}$$

where $\bar{c}$ is the average value of the constriction ratio. The total contact resistance is then given by

$$R = \frac{g(\bar{c})}{2\bar{a}Nk}. \tag{4}$$

The use of equation (4) requires a knowledge of N, the total number of contact spots, $\bar{a}$, the mean radius of the contact spots, and A_a, the actual contact area which are produced under a particular applied load. Values of these variables can be estimated from topographical data for the contacting surfaces and the mean plane separation, d, which depends upon the applied load and the physical properties of the materials in contact.

THE MODIFIED GREENWOOD AND WILLIAMSON CONTACT MODEL

In order to predict the thermal contact resistance across a pressed contact one must be able to estimate both the average size and the number of contacts as a function of load. Contact models have been created for this purpose. The Greenwood and Williamson (GW) elastic contact model [5], which is both moderately easy to implement and relatively accurate, will now be summarized.

The original GW model applies to the contact of two flat elastic planes, one of which is rough and the other of which is smooth; however, the model is readily adapted to the more general case of two rough surfaces [17, 18]. In this case, the equivalent, or sum surface, spectral moments equal the sums of the respective moments of the contacting surfaces.

In the GW model the rough surface is assumed to be covered with spherical asperities. It is further assumed that all of the asperities have the same radius r. The summit heights are considered to vary randomly. Summits are presumed to be uniformly distributed over the rough surface with a known density D_{sum} per unit nominal contact area.

The mean summit height lies above the mean surface height by an amount $\bar{z}_s$. The summit heights, z_s, measured relative to the mean summit height are assumed to follow a Gaussian distribution with a standard deviation σ_s.

McCool has used the random process model of rough surfaces to modify the GW contact model [6]. The random process model of rough surfaces can be used to relate D_{sum} and σ_s to m_0, m_2 and m_4, respectively the zero, second and fourth moments of the power spectral density of a surface profile:

$$D_{sum} = \frac{1}{6\pi\sqrt{3}}\frac{m_4}{m_2} \tag{5}$$

$$\sigma_s^2 = \left(1 - \frac{0.8968}{\alpha}\right)m_0. \tag{6}$$

The mean summit curvature averaged over all summit heights was determined by Bush *et al.* [19] to be

$$\kappa_m = \frac{8\sqrt{m_4}}{3\sqrt{\pi}}. \tag{7}$$

It will be assumed that all asperities are spherical with a radius given by

$$r = \frac{1}{\kappa_m} = \frac{3\sqrt{\pi}}{8\sqrt{m_4}}. \tag{8}$$

These relationships can be utilized in conjunction with the Greenwood and Williamson elastic contact model to develop the equations required for the prediction of the thermal contact conductance across a given pressed contact in a vacuum environment. The derivation of the requisite equations is presented in refs. [6, 20]. The equations will be presented without derivation in what follows.

The first step is the determination of the non-dimensional separation, d/σ_s, of the two contacting surfaces. Using Hertzian theory for the contact of a sphere and a flat one obtains

$$\frac{d}{\sigma_s} = F_{3/2}^{-1}\left(\frac{30.03W}{A_n E^*[\alpha - 0.8968]^{3/4} m_2^{1/2}}\right) \tag{9}$$

where W is the applied compressive force, A_n is the nominal contact area, d is the separation of the summit mean planes, E^* is the equivalent Young's modulus and α $(=m_0 m_4/m_2^2)$ is the bandwidth parameter. Through this text, $F_n(d/\sigma_s)$ is defined as

$$F_n = \int_{d/\sigma_s}^{\infty} (x - d/\sigma_s)^n \phi(x)\, dx \tag{10}$$

where $\phi(x)$ is the standard normal distribution function.

The next step is the determination of the actual contact area. Using Hertzian theory one can determine the actual area of contact to be given by

$$A_a = 0.06396(\alpha - 0.8968)^{1/2} A_n F_1(d/\sigma_s). \tag{11}$$

Once the actual contact area is determined the average value of the ratio of microcontact radius to flux tube radius, $\bar{c}$, can be determined from

$$\bar{c} \cong \left(\frac{A_a}{A_n}\right)^{1/2}. \tag{12}$$

The number of contacts can be evaluated from the assumed summit height distribution:

$$N = 0.03063\frac{m_4}{m_2} A_n F_0(d/\sigma_s). \tag{13}$$

Finally, the average contact radius, $\bar{a}$, can be evaluated using

$$\bar{a} = \left(\frac{3}{8}\right)^{0.5}\left(\frac{\pi m_0}{m_4}\right)^{0.25}\left(1 - \frac{0.8968}{\alpha}\right)^{0.25}\frac{F_{1/2}(d/\sigma_s)}{F_0(d/\sigma_s)}. \tag{14}$$

The values $F_n(d/\sigma_s)$ can be evaluated using numerical integration. The contact parameters required for the calculation of the TCR across a pair of pressed surfaces can be determined using the above relations.

Strongly anisotropic surfaces, or equivalently, sur-

faces possessing elliptical anisotropy, are surfaces characterized by a pronounced grain or lay [21, 22]. Ground surfaces are examples of strongly anisotropic surfaces.

Sayles and Thomas [21] concluded that equivalent values of m_2 and m_4 can be defined as follows:

$$m_{2e} = (m_{02}m_{20})^{1/2} \tag{15a}$$

$$m_{4e} = (m_{04}m_{40})^{1/2}. \tag{15b}$$

It then follows that an equivalent bandwidth parameter can be defined as

$$\alpha_e = \frac{m_0 m_{4e}}{m_{2e}^2} = \frac{m_0(m_{04}m_{40})^{1/2}}{m_{02}m_{20}}. \tag{16}$$

These equivalent surface parameters can be used in conjunction with the GW model. Thus, the GW model is readily expanded for the analysis of strongly anisotropic surfaces.

The Greenwood and Williamson model, as modified by the random process model of rough surfaces, is reported to be a reasonably accurate method of analyzing the elastic contact of rough surfaces. Although the model breaks down if a significant amount of plastic flow occurs, many tribological phenomena involve a large number of repeated contacts. In this case the assumption of elastic deformation should not be a problem.

The GW model can be used to determine the parameters required for predicting the thermal contact resistance across a pressed contact in a vacuum environment. The assumption of elastic contact represents a problem if one is considering the thermal contact resistance of a pressed contact undergoing its first load cycle. In this case one might expect the small surface asperities to undergo relatively large amounts of plastic deformation. Despite its limitations, the modified GW model may prove useful in the prediction of the thermal contact resistance across pressed contacts. The model will be employed in conjunction with the experimental portion of this research.

EXPERIMENTAL PROCEDURE

Thermal contact resistance data were obtained for ten pairs of pressed metal contacts. All measurements were made while the contacts were within a vacuum chamber. Figure 1 shows a schematic of the test chamber.

Contact resistance values were obtained as a function of contact pressure, surface texture and material properties. The test apparatus has been discussed in depth by McWaid [20]. Only the most important aspects of the experiment will be discussed below.

The heat flow through the column was maintained at about 7 W for the experiments on aluminum specimens and at about 3 W for the experiments on stainless steel specimens. A constant temperature bath was utilized to remove the energy from the bottom of the test column.

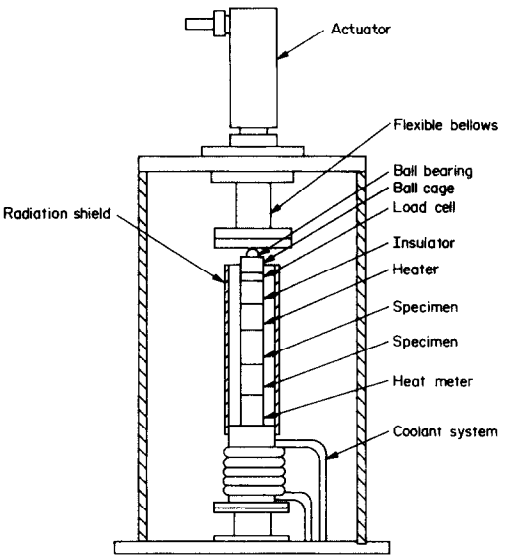

FIG. 1. Test assembly.

Intrinsic to the measurements of the thermal contact resistance values was the assumption that the heat transfer was one-dimensional through the specimens. A radiation shield was utilized to minimize the transverse radiative heat loss.

The radiation shield could be threaded onto the OFHC copper base, thus ensuring that its temperature remained close to that of the specimens. Thermocouples attached to the radiation shield allowed one to monitor the shield's temperature.

The insulator (see Fig. 1) was used to minimize the amount of heat transferred up through the bellows and hydraulic cylinder. The insulator was fabricated out of Vespel, a material possessing an extremely low thermal conductivity value. The thermal path downward through the specimens represented a much smaller thermal resistance than did the thermal path upward through the ball cage, ball, and bellows.

A heat meter was fabricated and used in order to measure the actual heat flow rate through the column. The heat meter was fabricated from NIST Standard Reference Material (SRM) 1462. SRM 1462 is an austenitic stainless steel with known thermal conductivity from 2 to 1200 K.

Three thermocouples were mounted into the heat meter at known axial locations. The heat flux, and thus the heat flow, through the meter was easily found using the one-dimensional Fourier equation. The heat flow through the meter, located below the lower specimen, was compared to the power input via the heater and the load cell, both located above the upper specimen. In the case of zero transverse and upward heat flow these numbers would be the same. In actuality, a small amount of energy would be conducted out of the top of the chamber. The heat flow through the specimens was also calculated using the specimens themselves as heat flow meters.

Small thermocouples were used in order to minimize conduction through the thermocouple leads, allow accurate specification of thermocouple location, and to minimize the disturbance of the heat flow. Thirty-six AWG thermocouples (0.013 cm = 0.005 in. diameter leads) were used throughout the study. The thermocouples were all at least 76 cm (30 in.) long. This relatively long length served to minimize conduction through the leads.

The thermocouples were mounted in holes drilled perpendicular to the axis of symmetry of the specimens and the heat meter. Each hole was approximately 0.508 cm (0.200 in.) deep, with a diameter just large enough to accommodate the thermocouple (approximately 0.051 cm = 0.020 in.). The thermocouples were mounted into the holes using a silver-filled epoxy. The epoxy has a relatively high thermal conductivity, thus ensuring that high temperature gradients did not exist through the bond lines. The thermocouples were wrapped partially around the specimen (or heat meter), and secured using a small piece of Kapton tape. Kapton tape possesses an extremely small thermal conductivity. Thus use of the tape for stress relief of the thermocouples did not affect the temperature distribution through the specimens (or heat meter).

The heat loss from the test column could be estimated by performing an energy balance on the system. The difference between the heater and load cell power dissipations, and the heat flowing through the heat meter, equalled the sum of the various heat losses from the system. The largest measured total heat loss was 2%.

Twenty specimens were studied. Each specimen was 3.81 cm (1.50 in.) long by 2.54 cm (1.00 in.) in diameter. Ten of the specimens were fabricated out of aluminum 6061-T6. The remaining ten specimens were fabricated out of 304 stainless steel. These two materials were chosen for several reasons. First, the stainless steel is quite hard, while the aluminum is relatively soft. Second, the thermal conductivity of the steel is much less than that of the aluminum. Finally, both materials are commonly used; thus, their mechanical and thermal properties are well known and readily available. The relevant material properties are presented in Table 1.

Two different types of finishes were studied. Some surfaces were bead-blasted such that a one-dimensional isotropic surface possessing a Gaussian distribution of heights, slopes and curvatures would result. Other surfaces were left as ground. These surfaces possessed a distinct lay; their surface textures were strongly anisotropic.

Table 1. Material properties

Material	Young's modulus† (GPa)	Thermal conductivity† ($W\ m^{-1}\ K^{-1}$)	Poisson's ratio‡
Al 6061-T6	67 (10.3 Mpsi)	200	0.33
CRES 304	270 (30 Mpsi)	16	0.30

† The values of Young's modulus and thermal conductivity were obtained from ref. [9]. They correspond to a temperature of about 35°C.

‡ The values of Poisson's ratio were obtained from ref. [2].

For both of the materials studied three pairs of specimen surfaces were prepared by bead blasting. These surfaces were bead blasted using either relatively small glass beads (0.0089–0.015 cm diameter), medium-sized glass beads (0.0178–0.0249 cm diameter) or relatively large beads (0.0406–0.0432 cm diameter). In all instances, the contacting specimens were of the same material and surface finish.

The ground surfaces were used as follows. One pair of ground aluminum specimens were placed together such that their lays were parallel. The second pair of ground aluminum specimens were placed together such that their lays were perpendicular. The same procedure was followed with the ground steel specimens.

The test procedure will now be discussed. All experiments were performed using this same basic procedure.

Contact resistance data were obtained for pressures between 0.16 MPa (23 psi), corresponding to a zero hydraulic gauge pressure, and about 6.9 MPa (1000 psi). Data were obtained both for first loading, that is for monotonically increasing pressures from 0.16 MPa up to the maximum pressure, and for the unloading cycles. Sequential measurements were made at pressures about 0.69 MPa above or below the previous test pressure.

Eight to ten hours of actual testing were required to obtain the data for each pair of specimens. The test column was allowed to equilibrate after each load change. Equilibrium was assumed to have been reached when none of the measured temperatures in the test column deviated by more than 0.1°C over a 5 min period.

While *any* measurable temperature change implies that an equilibrium condition has not been reached, Antonetti and Eid [23] have reported that the steady-state value of the thermal contact resistance is reached relatively quickly in comparison to the system as a whole. This is due to the relatively small thermal capacitance of the solid–solid interface. Indeed, Antonetti and Eid report that the time required to determine the actual contact resistance should be less than 10 min for measurements being made after changing only the mechanical load by an incremental amount (as was done in this series of experiments).

The assumption of steady-state corresponding to a maximum temperature change of not more than 0.1°C over 5 min resulted in a 'transient' period of between 10 and 50 min for the experiments reported herein. Thus, the fact that true steady-state was not reached between load changes should not have introduced significant errors into the measurements. This point will be discussed in more depth in the Results section.

Temperatures were written to a floppy disk every 5

min during each experiment. The gauge pressure as well as the current and voltage drop across the heater were input to the computer, and subsequently written to disk, after steady-state had been reached.

The modified Greenwood and Williamson model, as presented above, has been used to predict the thermal contact conductance across the experimental specimens. The predicted and measured values of the contact conductance have been compared, thereby allowing one to gauge the applicability of the contact model.

The first step in the prediction of the TCR across a given pressed contact is the evaluation of the texture parameters of the contacting surfaces. In particular, the zero, second and fourth spectral moments must be evaluated. A surface profilometer was used to characterize the surfaces used in this research.

Each of the contacting surfaces was characterized using the same basic technique. A Dektak 3030 Auto II Profile Measuring System was used to obtain the surface data. A sampling interval of 2.5 μm was used. Each profile trace was comprised of 2000 data points. Thus the scan length of each trace was 5 mm. The radius of the diamond stylus was 2.5 μm. A force of 30 g was used to ensure contact between the stylus and the surface being measured. All height measurements were made in angstroms; the height readings were written to computer data files for subsequent analysis.

Two traces were used to characterize each of the bead-blasted surfaces. These traces were made in different areas of the surface; moreover, the two traces were made at right angles to one another. Each profile was analyzed independently; the spectral moments were determined for each profile. The resulting moments were then averaged. The average values of the two data sets were used to represent the surface.

The ground surfaces were characterized by four traces of the profilometer. Two traces were taken parallel to the surface lay, and two traces were taken perpendicular to the surface lay. Again, the spectral moments were evaluated from each profile. The average of the two sets of moments obtained from the profiles taken parallel (perpendicular) to the lay were used to represent the surface texture parallel (perpendicular) to the lay.

The first step in the evaluation of the surface parameters was the determination of the mean profile height. A least squares line was fit to each set of data (each individual trace). This line constituted the mean profile height. No long-wavelength filtering was used since the long wavelength irregularities can play a critical role in determining the thermal contact resistance across a pressed contact [11].

The minimum resolvable frequency of a sampling process equals twice the sampling interval. Thus, each profile was subject to a short-wavelength cut-off of 5 μm. There is no physical significance with regards to thermal contact resistance corresponding to this short-wavelength limit.

A short-wavelength cut-off relevant to the phenomenon of contact resistance may exist; however, such a limit has not yet been determined. The choice of short-wavelength cut-off might have significant ramifications in the evaluation of the second and fourth moments (and thus the bandwidth parameter) of the profile power spectral density curve. Sayles and Thomas [24] have reported that m_2 and m_4 can increase without bounds as the sampling interval is reduced to zero.

A parametric study has been performed on the surfaces studied herein in the hope of deducing the sensitivity of the calculated thermal contact resistance on the sampling interval. The profile moments and bandwidth parameter have been evaluated using intervals ranging from 2.5 μm up to 25 μm. As previously mentioned the surface data were obtained using a sampling interval of 2.5 μm. Thus, the sampling interval could effectively be increased by considering every other, every third, or every nth data point. This was the technique used.

The following parameters were determined for the steel surfaces bead-blasted with the smallest beads (SF1 and SF2) and two of the ground aluminum surfaces (AG3 and AG4): m_0, m_2, m_4, and α. The resulting values for the steel specimens are presented in Table 2. The evaluation of the spectral moments has been discussed in ref. [20].

Although the parameters do change with the sampling interval, the changes are not too extreme. The question now becomes how sensitive is the calculated thermal contact resistance to small changes in the surface parameters?

The Greenwood and Williamson elastic contact model was used to determine the thermal contact conductance as a function of the sampling interval. The surface parameters were substituted into the appropriate equations to yield the contact conductance as a function of sampling interval. The results for SF1 and SF2 are shown in Fig. 2. The conductance values calculated using the intermediate values of sampling interval fall between the limiting cases shown in Fig. 2.

The calculated contact conductance varied by less than 15% as the sampling interval was varied between 2.5 and 25 μm. These results help to alleviate the problems associated with the short-wavelength filtering of the surface data. As long as a reasonable sampling interval is used the errors introduced in the evaluation of the surface spectral moments will probably be less than the errors inherent to the mechanical

Table 2. Sum surface spectral moments as a function of sampling interval for surfaces SF1 and SF2

Sampling interval (μm)	2.5	5.0	10	15	25
m_0 (μm^2)	0.77	0.78	0.73	0.67	0.62
m_2	0.0093	0.0084	0.0082	0.0082	0.0078
m_4 (μm^{-2})	0.00065	0.00057	0.00057	0.00060	0.00056
α	5.79	6.30	6.19	5.98	5.71

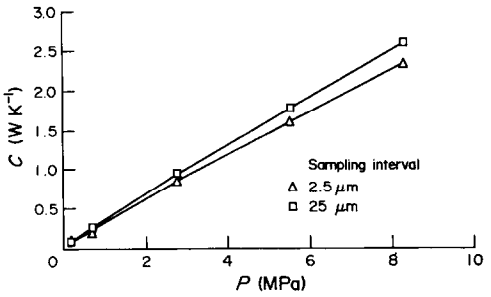

FIG. 2. Contact conductance C vs contact pressure P as a function of sampling interval for steel surfaces SF1 and SF2.

model of the contacting surfaces. This conclusion should be caveated by pointing out that the evaluation of the parameters of some types of surface finishes may be much more sensitive to the choice of sampling interval than the surfaces considered herein (see ref. [24], for example).

All of the surface parameters used in the theoretical prediction of the thermal contact resistances across the experimental specimens were evaluated using a sampling interval of 2.5 μm. The resulting spectral moments are presented in Table 3.

RESULTS

The thermal contact conductance across a given contact was readily determined from the experimental data. The defining equations for the thermal contact resistance and conductance have already been presented. The heat flux through the specimens was the most difficult parameter to measure.

The heat flow across the interface could be measured using three distinct methods. The power dissipation by the heater and load cell were measured; the sum of these power dissipations equals the power input into the test column. Also, as discussed above, a heat meter was constructed so as to allow the determination of the heat flow out of the test column. The final method of determining the heat flow through the test column was to use the specimens themselves as heat meters.

In practice two different methods were employed to evaluate the heat flow used in the calculation of the contact resistance. The aluminum specimens possess a high value of thermal diffusivity. Consequently the test column reached equilibrium relatively quickly during experiments involving aluminum specimens. During tests of aluminum specimens the value of the heat flow calculated from the power dissipations of the heater and the load cell agreed to within about 2% with the value of heat flow calculated using the heat meter. This being the case, the value of heat flow determined using the heat meter was used in the calculations of the TCR across the aluminum specimens.

Table 3. Sum surface texture parameters

Surface pair	m_0 (μm^2)	m_2	m_4 (μm^{-2})	α
AF1/AF2	6.81	0.0522	0.00291	7.27
SF1/SF2	0.765	0.00933	0.000654	5.70
SG1/SG2	1.014	0.00740	0.00103	19.1
SG3/SG4	0.702	0.00248	0.000224	25.6

The thermal diffusivity of stainless steel is relatively low. Thus, the test column required a relatively long period of time to equilibrate after each load change during experiments on the steel specimens. As previously mentioned, Antonetti and Eid [23] have reported that since the thermal capacitance of a pressed contact is small, the value of the thermal contact resistance reaches equilibrium much more rapidly than does a typical test column designed to measure the resistance. Turyk and Yovanovich [25] also support this conclusion.

This being the case, experiments on the steel specimens were terminated before the whole test column had equilibrated. Antonetti and Eid have demonstrated that when such a procedure is followed the contacting specimens should be used to monitor the heat flow across the contact. This is what was done in this study. The value of the heat flow used in the determination of the thermal contact resistance of the contacting steel specimens was found by averaging the heat flows through the two specimens.

Only the results for four of the ten specimen pairs will be presented. Results will be presented for the steel surfaces bead-blasted with the smallest beads (SF1 and SF2), the aluminum surfaces bead-blasted with the smallest beads (AF1 and AF2) and the ground steel specimens (SG1/SG2 and SG3/SG4). SG1/SG2 were oriented with their lays parallel; SG3/SG4 were oriented with their lays perpendicular.

Figures 3–6 present plots of the measured and predicted values of TCC as a function of the nominal contact pressure for the four specimen pairs specified above. The first loading data correspond to the first load cycle seen by the contacting surfaces. Some degree of plastic deformation of the contacting asperities is expected to occur during the first load

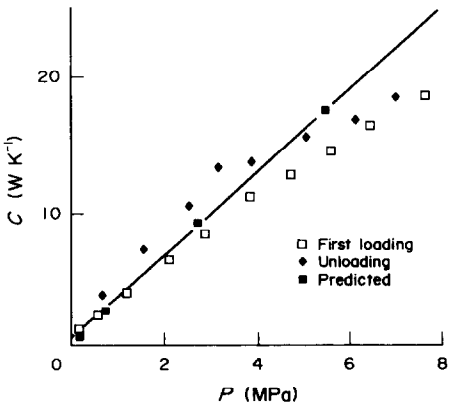

FIG. 3. Contact conductance C vs contact pressure P for aluminum surfaces AF1 and AF2.

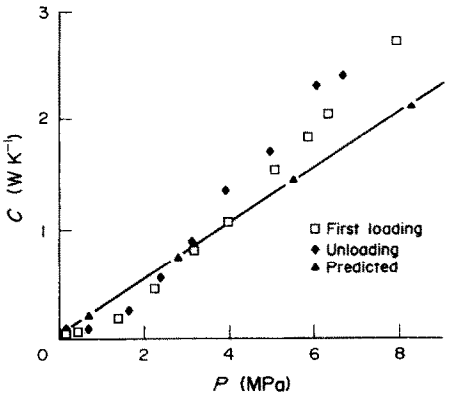

Fig. 4. Contact conductance C vs contact pressure P for steel surfaces SF1 and SF2.

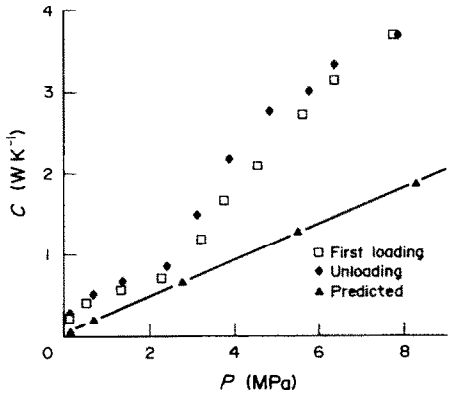

Fig. 5. Contact conductance C vs contact pressure P for steel surfaces SG1 and SG2.

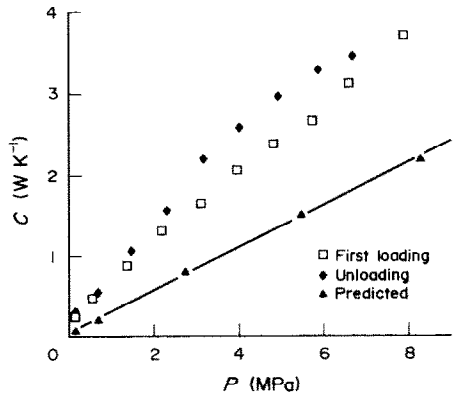

Fig. 6. Contact conductance C vs contact pressure P for steel surfaces SG3 and SG4.

cycle. Conversely, one would expect the contacting asperities to recover elastically during unloading.

The expected hysteresis is apparent in the figures. The contact conductance at a given pressure is greater during unloading than during the first load cycle. The highest, sharpest asperities are plastically deformed during the first load cycle. Consequently the contact area, and the contact conductance, at a given pressure are greater during unloading. The hysteresis observed in the figures is not too great; however, one would expect that the divergence of the first loading and the unloading curves would increase as the maximum applied pressure is increased.

This hysteresis can be used to practical advantage. One can maximize the thermal contact conductance across a given joint by preloading the faying surfaces of the joint as much as possible before the final joint is made.

The third data set presented in each figure corresponds to the predicted contact conductance for the applicable pair of specimens. A least squares line has been fit to the predicted values. The figures illustrate that the predicted conductance increases nearly linearly with contact pressure.

Insight into the applicability of the modified Greenwood and Williamson elastic contact model with regards to the contact of strongly anisotropic surfaces can be gained by comparing the data for the ground steel specimens.

Although the theory was much less accurate at predicting the conductance across the ground steel surfaces than across the bead-blasted steel surfaces, it was surprisingly successful. The measured conductance values are greater than the predicted values for all pressures for both specimen pairs; however, the differences are relatively small.

One would expect that the theory would be more successful at predicting the contact conductance across the bead-blasted surfaces since the contact of the ground surfaces (strongly anisotropic) was modeled as the contact of an equivalent isotropic surface against a plane. The GW model does not differentiate between two contacting ground surfaces whose lays are parallel and two contacting ground surfaces whose lays are perpendicular.

As mentioned in the Introduction, many researchers have studied contact resistance. This being the case, a large amount of TCR data has been presented in the literature. Unfortunately, many different methods have been employed in an effort to quantify the surface texture of the contacting surfaces. The authors were not able to find published TCR/surface texture data that allow the direct use of the equations presented above. Snaith *et al.* have reviewed several correlations [9]. They have used these correlations to estimate the contact conductance across both aluminum 6061-T6 and stainless steel 304 specimens. The contact conductance values reported herein fall between the conductance values obtained using the reported correlations.

UNCERTAINTY ANALYSIS

The accuracy of the measured contact resistance values will now be estimated. The thermocouples were all the same type; moreover, all of the thermocouples were obtained from the same vendor. This being the case, although the absolute temperature values may

not be extremely accurate, the temperature differences, which are what were utilized in this research, should be accurate to within about 0.05 K. The predominant sources of error involve the thermocouple locations and the magnitude of the heat flow through the test column.

The thermocouple holes were located axially to within 0.005 cm (0.002 in.) of the nominal hole location. The holes were approximately 0.013 cm (0.005 in.) larger in diameter than the thermocouples. Thus, the maximum off-set from the nominal position was about 0.011 cm (0.0045 in.).

The second major error source involves the quantification of the heat flow through the column. As already discussed, the heat flow was known to within 2% during tests involving the aluminum specimens.

The specimens were used to quantify the heat flow during experiments on the stainless steel specimens. Since the value of the specimen conductivity was obtained from the literature, the heat flows are probably known to within only about 5% of the calculated values.

Based on the above reasoning, the largest uncertainty would be associated with either the aluminum or steel specimen pairs that were bead-blasted with the smallest beads. The maximum uncertainty corresponds to the highest load across the smoothest specimens, since these conditions result in the smallest temperature drop across the interface.

The largest uncertainty associated with the measurements on the smoothest aluminum specimens varies from $\pm 2.8\%$ at 0.157 MPa to $\pm 18\%$ at 7.61 MPa. The largest uncertainty associated with the measured resistance values across the smoothest steel surfaces varies from $\pm 5.8\%$ at 0.157 MPa to $\pm 32\%$ at 7.98 MPa. All pressures are believed to be accurate to within 2% of the stated values.

SUMMARY

Thermal contact resistance has been the topic of many research efforts. Most of the contemporary models are based on the assumption that contacting asperities undergo plastic deformations. While deformation during the first few load cycles may be predominantly plastic, a state of elastic deformation should be reached after a number of load cycles.

A modified version of the Greenwood and Williamson elastic contact model has been developed for use in the prediction of the TCR across pressed metal contacts in a vacuum environment. The requisite surface parameters can be calculated from the output of a standard stylus profilometer; moreover, only commonly known material properties such as the Young's modulus, Poisson's ratio and thermal conductivity are required to use the model.

The thermal contact conductance across ten pairs of surfaces in a vacuum environment has been measured as a function of contact pressure. The theory presented in this paper has been used to predict the thermal contact conductance as a function of contact pressure for each pair of specimens. The measured and predicted values have been presented and compared.

The predictions agree relatively well with the measurements. The worst-case error was about 75% of the measured value. In general, however, the error was less than 25% of the measured value.

Thus, the theory presented herein constitutes a viable tool for the heat transfer analyst. The theory is relatively easy to implement and the results are reasonably accurate.

Acknowledgements—This work was supported by the Santa Barbara Research Center and the State of California through a MICRO Grant. The authors would like to thank Mr Randy Page of Sloan Technology for the use of the Dektak 3030 Auto II Profile Measuring Systems.

REFERENCES

1. L. S. Fletcher, Recent developments in contact conductance heat transfer, *J. Heat Transfer* **110**(4-B), 1059–1070 (1988).
2. C. V. Madhusudana and L. S. Fletcher, Contact heat transfer—the last decade, *AIAA J.* **24,** 510–523 (1985).
3. M. M. Yovanovich, A. Hegazy and J. DeVaal, Surface hardness distribution effects upon contact, gap, and joint conductances, AIAA Paper No. 82-0887 (1982).
4. M. M. Yovanovich, A. H. Hegazy and V. W. Antonetti, Experimental verification of contact conductance models based upon distributed surface micro-hardness, AIAA Paper No. 83-0532 (1983).
5. J. A. Greenwood and J. B. P. Williamson, Contact of nominally flat surfaces, *Proc. R. Soc. Lond.* **A295,** 300–319 (1966).
6. J. I. McCool, Comparison of models for the contact of rough surfaces, *Wear* **107,** 37–60 (1986).
7. T. R. Thomas, *Rough Surfaces.* Longman, U.K. (1982).
8. R. G. S. Skipper and K. J. Wootton, Thermal resistance between uranium and can, *Proc. 2nd Int. Conf. on Peaceful Uses of Atomic Energy*, Geneva, Paper P/87 (1958).
9. B. Snaith, S. D. Probert and P. W. O'Callaghan, Thermal resistances of pressed contacts, *Appl. Energy* **22,** 31–84 (1986).
10. H. Fenech and W. M. Rohsenow, Prediction of thermal conductance of metallic surfaces in contact, *Trans. ASME, J. Heat Transfer* **85C,** 15–24 (1963).
11. A. M. Clausing, Thermal contact resistance in a vacuum environment, Ph.D. Thesis, Univ. of Illinois, U.S.A. (1963).
12. E. Fried, Thermal joint conductance in a vacuum, ASME Paper No. 63-AHGT-18 (1963).
13. L. S. Fletcher, Thermal contact resistance of metallic interfaces: an analytical and experimental study, Ph.D. Thesis, Arizona State Univ., U.S.A. (1969).
14. L. C. Roess, Theory of spreading resistance, Appendix A of Report of Beacon Lab. of Texas Inc., Beacon, New York, unpublished (1949).
15. B. B. Mikic and W. M. Rohsenow, Thermal contact resistance, M.I.T. Report No. 4542-41 (1966).
16. M. G. Cooper, B. B. Mikic and M. M. Yovanovich, Thermal contact conductance, *Int. J. Heat Mass Transfer* **12,** 279–300 (1969).
17. M. O'Callaghan and M. A. Cameron, Static contact under load between nominally flat surfaces in which deformation is purely elastic, *Wear* **36,** 79–97 (1976).
18. H. A. Francis, Application of spherical indentation mechanics to reversible and irreversible contact between rough surfaces, *Wear* **45,** 221–269 (1977).
19. A. W. Bush, R. D. Gibson and G. P. Keogh, The limit

of elastic deformation in the contact of rough surfaces, *Mech. Res. Commun.* **3**, 169–174 (1976).
20. T. H. McWaid, Thermal contact resistance across pressed metal contacts in a vacuum environment, Ph.D. Dissertation, Univ. of California at Santa Barbara, U.S.A. (1990).
21. R. S. Sayles and T. R. Thomas, Thermal conductance of a rough elastic contact, *Appl. Energy* **2**, 249–267 (1976).
22. A. W. Bush, R. D. Gibson and G. P. Keogh, Strongly anisotropic rough surfaces, *Trans. ASME, J. Lubrication Technol.* **101**, 15–20 (1979).
23. V. W. Antonetti and J. C. Eid, A technique for making rapid thermal contact resistance measurements, *Proc. Int. Symp. on Cooling Technology for Electronic Equipment*, Honolulu, HI, March, pp. 449–460 (1987).
24. R. S. Sayles and T. R. Thomas, Measurements of the statistical microgeometry of engineering surfaces, *Trans. ASME, J. Lubrication Technol.* **101F**, 409–418 (1979).
25. P. J. Turyk and M. M. Yovanovich, Transient constriction resistance for elemental flux channel heated by uniform sources, ASME Paper No. 84-HT-52 (1984).

RESISTANCE THERMIQUE DE CONTACT ENTRE METAUX COMPRIMES DANS UN VIDE AMBIENT

Résumé—La conductance thermique de contact est mesurée en fonction de la pression de contact pour dix paires de surfaces sur un vide environnant. Une version modifiée du modèle de contact élastique selon Greenwood et Williamson a été utilisée pour prédire la conductance de contact. Les valeurs mesurées et prédites sont présentées et comparées. L'écart est généralement inférieur à 25% pour les surfaces isotropiquement rugueuses et inférieur à 50% pour les surfaces fortement anisotropes. Ainsi la théorie présentée constitue un outil viable pour une analyse du transfert thermique. La théorie est relativement facile à exploiter et les résultats sont raisonnablement précis.

THERMISCHER KONTAKTWIDERSTAND ÜBER VERPRESSTE METALLISCHE KONTAKTE IN EINER EVAKUIERTEN UMGEBUNG

Zusammenfassung—Die thermische Kontaktleitfähigkeit wird in Abhängigkeit vom Kontaktdruck für 10 Oberflächenpaarungen in einer evakuierten Umgebung gemessen. Zur Vorausberechnung der Kontaktleitfähigkeit in Abhängigkeit vom Kontaktdruck für jede einzelne Paarung wird eine modifizierte Version des elastischen Kontaktmodells nach Greenwood und Williamson benutzt. Gemessene und berechnete Werte werden vorgestellt und verglichen. Die Rechenwerte weichen im allgmeinen für isotropisch rauhe Oberflächen um weniger als 25% von den Meßwerten ab, bei stark anisotropen Oberflächen sind dies 50%. Die vorgestellte Theorie erweist sich auf diese Weise als ein sinnvolles Werkzeug für die Analyse des Wärmeübergangs. Sie ist relative einfach anzuwenden, und die Ergebnisse zeigen brauchbare Genauigkeit.

ТЕПЛОВОЕ КОНТАКТНОЕ СОПРОТИВЛЕНИЕ В МЕТАЛЛИЧЕСКИХ КОНТАКТАХ ПОД ДАВЛЕНИЕМ В УСЛОВИЯХ ВАКУУМА

Аннотация—Измерялась контактная теплопроводность как функция давления для десяти пар поверхностей в условиях вакуума. Для определения контактной теплопроводности каждой пары образцов применялся модифицированый вариант модели упругого контакта Гринвуда и Вильямсона. Приводятся и сравниваются экспериментальные и расчетные результаты. Расхождение между ними составляет приблизительно 25% в случае изотропных шероховатых поверхностей и 50% для сильно анизотропных поверхностей. Изложенная теория представляет собой эффективный способ анализа теплопереноса. Она относительно проста в использовании, и полученные на ее основе результаты являются достаточно точными.